Journal of Hazardous Materials 161 (2009) 1087–1094

Contents lists available at ScienceDirect

Journal of Hazardous Materials

journal homepage: www.elsevier.com/locate/jhazmat

Determination of adsorptive properties of a Turkish Sepiolite for removal of Reactive Blue 15 anionic dye from aqueous solutions

A. Tabak[a,*], E. Eren[b], B. Afsin[c], B. Caglar[c]

[a] Department of Chemistry, Faculty of Arts and Sciences, Rize University, 53100 Rize, Turkey
[b] Department of Chemistry, Faculty of Arts and Sciences, Ahi Evran University, 40100 Kirsehir, Turkey
[c] Department of Chemistry, Faculty of Arts and Sciences, Ondokuz Mayis University, 55139 Kurupelit-Samsun, Turkey

ARTICLE INFO

Article history:
Received 1 August 2007
Received in revised form 18 April 2008
Accepted 18 April 2008
Available online 23 April 2008

Keywords:
Reactive Blue 15
Adsorption
Zeolitic water
Sepiolite
Turkey

ABSTRACT

Reactive Blue 15 (RB 15) adsorption on the Turkish Sepiolite was carried out by batch equilibrium technique. IR spectrum and surface area measurement of the composite of dye-sepiolite (Turkish) pointed out that dye species replaced partly the zeolitic water to form hydrogen bond with bound water and adsorbed to the channels sites. The effects of temperature, pH and ionic strength on adsorption of dye molecules were investigated and the nature of adsorption process was determined by calculating ΔH, ΔS and ΔG values. The adsorbed amount increased with increase in temperature, but that for high pH values decreased for the adsorption of reactive dye.

© 2008 Elsevier B.V. All rights reserved.

1. Introduction

The colourants have been used for painting and dyeing of surrounding, skin and cloth by people since the beginning of humankind and they were from natural origin until 19th century. Recent statistics have shown that the production and consumption of dyes in the world have arrived about 700,000 tonnes [1]. Dyes containing chromophores and auxochromes groups can be classified as reactive, metal complex, acid, direct, basic, disperse, pigment, mordant, vat, sulphur, anionic, solvent, ingrain and others. The most of the reactive dyes including a reactive group such as vinyl sulphone are azo or metal complex azo compounds and interact with cotton, wool, etc., to form covalent bond. The release of these dyes, which have the lower degree of fixation due to hydrolysis of reactive groups in the water phase, into the environment is undesirable.

Generally, physicochemical and biological methods such as precipitation, flotation, ion exchange, adsorption, oxidation and, bacterial and fungal biosorption and biodegradation (aerobic, anaerobic and anoxic) can be employed to remove colour from dye containing wastewaters [2,3].

The photocatalytic degradation, microemulsions and biological techniques were applied to reduce azo dye effects in the wastewater [4–6]. However, the many researchers have focused on the other alternatives [7–10] because the economically feasible of the process employed is very important. For this purpose, the cheap and efficient alternate materials including clays as sepiolite, etc., are used because of their high-specific surface area, high adsorption capacity, microporous structure. The sepiolite is a clay mineral with an ideal formula $Mg_8Si_{12}O_{30}(OH)_2$ and also the unit cell of the sepiolite corresponding to the orthorhombic system consists of microchannels [11–13]. This mineral is commonly used as adsorbents, fillers, colour changing agent, catalyst or catalyst supports [14–16].

Mobile cations in the SiO_4 tetrahedral sheet (Al^{3+} and Fe^{3+}) and MgO_6 octahedral sheet (Fe^{2+}, Fe^{3+}, Al^{3+}, Mn^{2+} and Ti^{2+}) and exchangeable ions (Ca^{2+} and Mg^{2+}), and variable amounts of zeolitic water in the ideally rectangular channels give rise to high surface areas and structural changes [11,13,16–18].

The behaviour of the sepiolite when treating with some organic molecules has been studied by the some researchers [17,19–21]. Sorption of organic molecules such as 15 Crown Ether 5, Crystal Violet, Methylene Blue on the sepiolite showed that there are free negative sorption sites (P^-) and neutral sorption sites (N) on its surface [20,22]. The studies of adsorption of monovalent and divalent organic cations on the sepiolite exhibited that monovalent organic

* Corresponding author. Tel.: +90 464 2236126-1265; fax: +90 464 2235376.
E-mail address: ahmtabak@hotmail.com (A. Tabak).

0304-3894/$ – see front matter © 2008 Elsevier B.V. All rights reserved.
doi:10.1016/j.jhazmat.2008.04.062

Table 1
Chemical composition of the Turkish Sepiolite

Constituents	Weight percent (%)
SiO_2	51.95
MgO	23.35
Al_2O_3	2.14
Fe_2O_3	0.41
Na_2O	0.22
K_2O	0.36
CaO	2.77
TiO_2	0.08
SO_3	0.52
Loss of ignition	18.46

cations may bind to charged and neutral sites of sepiolite but divalent organic cations bind to the charged sites only. However, there have not been any studies in the literature on the adsorption properties of Reactive Blue 15 (RB 15) dye on the Turkish Sepiolite.

In this work, our first purpose was to investigate the effects of temperature, pH and ionic strength on adsorption process of reactive dye on the Turkish Sepiolite which constitutes a part of the abundant sepiolite mineral reserves of Turkey. And second one is to enlighten the interactions between this dye molecule and the Turkish Sepiolite, using Fourier transform infrared spectroscopy (FTIR), the surface area measurements, and thermodynamic data.

2. Experimental

2.1. Materials

The sepiolite used was obtained from the Eskişehir region, in Turkey. The chemical composition of the Turkish Sepiolite is given in Table 1.

RB 15 dye used in this study was obtained from Sigma. The molecular structure of this dye is shown in Fig. 1.

2.2. Adsorption procedure

The natural Turkish Sepiolite was treated with distilled water to remove the soluble impurities before adsorption procedure. The obtained suspension was filtered and the supernatant was dried at 105 °C for 12 h. Adsorption experiments on the Turkish Sepiolite were made using the batch method. 100 mg of adsorbent and 50 ml of an aqueous solution of each dye in the concentration range (1.0×10^{-5} to 1.4×10^{-4} M) were put into plastic tubes and shaken rigorously in the different temperature intervals of 25, 35, 45 and 55 °C. Adsorption process to determine the final equilibrium was followed from 5 to 180 min. The effects of pH and electrolyte on the reactive dyes adsorption were determined over a range of pH from 2.5 to 9.5 and in the varying concentration of 0.1, 0.2, 0.3, 0.4 and 0.5 mol/L NaCl, respectively. After the adsorption equilibrium is reached, the suspensions were centrifuged at 15,000 rpm and the concentrations of adsorbed dyes were by the Unicam UV2 UV–vis spectrophotometer. The measurements were made at the wavelength λ_{max} = 675 nm for RB 15 dye.

The amounts of dye retained by the Turkish Sepiolite (q_e) were calculated by the following equation:

$$q_e = \frac{(C_0 - C_e)V}{W}$$

Here C0 and C_e are initial and equilibrium concentrations of dye solutions (mg/L), respectively, V are volumes of dye solutions and W is the mass of the Turkish Sepiolite used (g).

2.3. The measurement of surface charge

Surface charge of the sepiolite sample was measured in 50 cm^{-3} of 10^{-3}, 10^{-2} and 10^{-1} M NaCl solutions by potentiometric titration of the sepiolite suspension. The Turkish Sepiolite sample (0.4 g) was added to a given electrolyte solution and the suspension was equilibrated under N_2 at its natural pH for 4 h. The suspension was mixed with a magnetic stirrer and the temperature was maintained at 25 °C. Following equilibration, the pH value was adjusted by adding of 0.1 M HCl solution. Suspension was then titrated by the addition of 0.1 M NaOH solution. After each addition of a small amount base, it was stable for 5 min and pH was recorded. To check reversibility, suspension was back titrated with 0.1 M HCl solution [23].

2.4. The characterization of the Turkish Sepiolite

FTIR spectra of the untreated Turkish Sepiolite and Turkish Sepiolite-dye composite were recorded in the region 4000–200 cm^{-1} on a Mattson-1000 FTIR spectrometer at a resolution of 4 cm^{-1}. The bands in the IR spectrum of the untreated Turkish Sepiolite (Fig. 2) may be summarized as follows: (i) the band of the triple bridge group Mg_3OH is at 3697 cm^{-1}, (ii) the absorption of the structurally bound water is seen at 3591 cm^{-1} and (iii) the stretches at the 3620 and 3451 cm^{-1} and the OH-bending mode at 1660 cm^{-1} are associated with zeolitic water. The lattice vibrations are given as follows: (a) the Si–O combination bands at 1213, 1090 and 987 cm^{-1}, (b) the basal plane of the tetrahedral units exhibiting the Si–O–Si plane vibrations at 1019 and 474 cm^{-1}, (c) the feature at 442 cm^{-1} arising from the Si–O–Mg of the octahedral–tetrahedral linkage and (d) Mg_3OH-bending vibration at 655 cm^{-1} [11,24]. Dolomite impurities give rise to the 1440 cm^{-1} band [13].

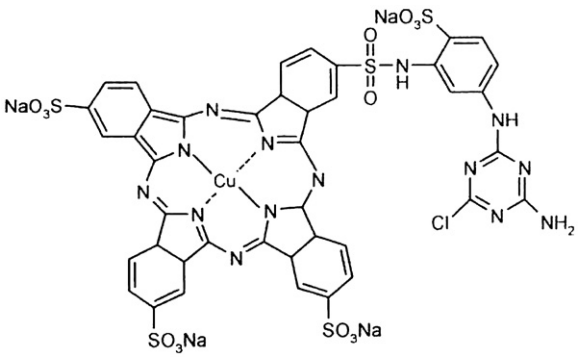

Fig. 1. The molecular structure of the RB 15 dye molecule.

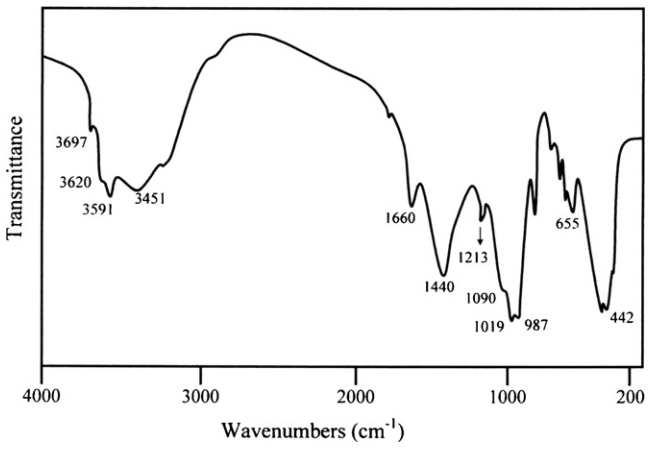

Fig. 2. FTIR spectrum of the Turkish Sepiolite.

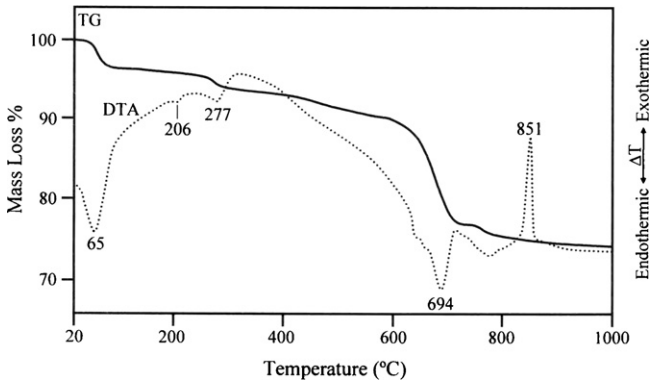

Fig. 3. Thermal analysis curve of the Turkish Sepiolite.

Table 2
Thermoanalytical data for the Turkish Sepiolite

Compound	Temperature range (°C)	Mass loss (%)	Total mass loss (%)
Turkish Sepiolite	20–105	1.92	
	180–232	0.60	
	232–326	1.79	
	580–725	13.21	17.52

Simultaneous TG and DTA analyses were carried out on a Rigaku TG 8110 thermal analyzer combined TAS 100 (range 25–100 °C) under nitrogen flow (80 ml min^{-1}) with a heating rate of 10 °C min^{-1}. The thermal behaviour of the Turkish Sepiolite is represented in Fig. 3 together with the mass losses in each stage in Table 2. Two endothermic peaks at 25–105 and 180–232 °C on the DTA curves of the Turkish Sepiolite corresponds to the removal of moisture and zeolitic water [19,25] which have mass losses by 1.92 and 0.60%, respectively. An endothermic peak at 232–326 °C which exhibit a mass loss by 1.79%, represents the desorption of bounded water. In addition, dehydroxylation process and decomposition of the dolomite impurity occur in the temperature ranges 580–720 and 725–823 °C which is followed by a phase change exothermic peak at 851 °C [19,21,24–26].

XRD pattern was traced on a Rigaku 2200 automated powder diffractometer using Ni filtered Cu Kα radiation (λ, 1.54050 Å). The Turkish Sepiolite was characterized by strong reflections at 7.04° and 7.12° (2θ) of d(1 1 0) and (0 0 1) values about 12.55 and 12.42 Å, respectively, and a weak reflection at about 19.6° 2θ and several very weak reflections (Fig. 4). However, XRD spectrum of the same sample showed strong peaks at 30.88° and 41.04° 2θ due to the dolomite impurity.

Surface areas for the untreated Turkish Sepiolite and Turkish Sepiolite-dye composite were measured by nitrogen adsorption at 77 K using Quantachromosorb.

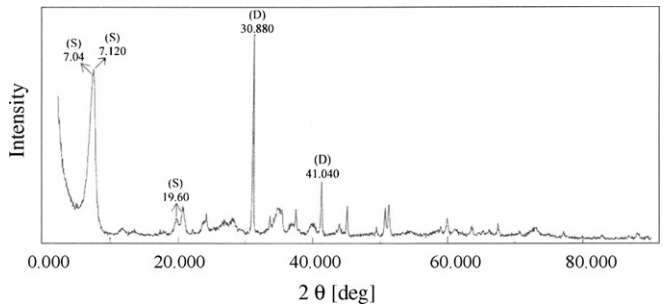

Fig. 4. XRD spectrum of theTurkish Sepiolite.

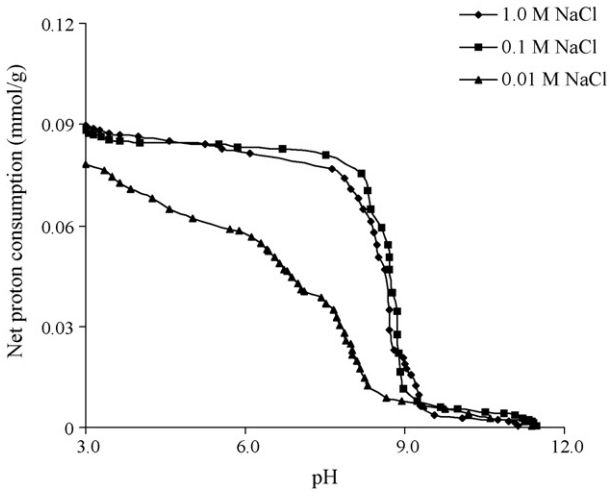

Fig. 5. Net proton consumption vs. pH curves of the untreated Turkish Sepiolite in NaCl solutions.

2.5. Surface properties of sepiolite sample from potentiometric titration

As is shown in Fig. 5, the interaction of the H^+ and OH^- ions with the Turkish Sepiolite surface was reflected in the shift of the titration curves in electrolyte solutions of NaCl. The titration curves of sepiolite sample at different ionic strengths were not display a common intersection point. Instead, the curves are parallel and shifted towards lower pH at higher ionic strength. This trend observed on the Na-MX80 montmorillonite in continuous titrations [27]. Recent papers [28–31] have shown that the absence of common intersection point can be explained by direct or indirect effects of the structural charge on the dissociation of the edge sites and dissolution of minerals.

3. Results and discussion

3.1. Adsorption model

The Langmuir and Freundlich isotherm models were applied to the experimental data (Figs. 6 and 7). The data confirm the linear

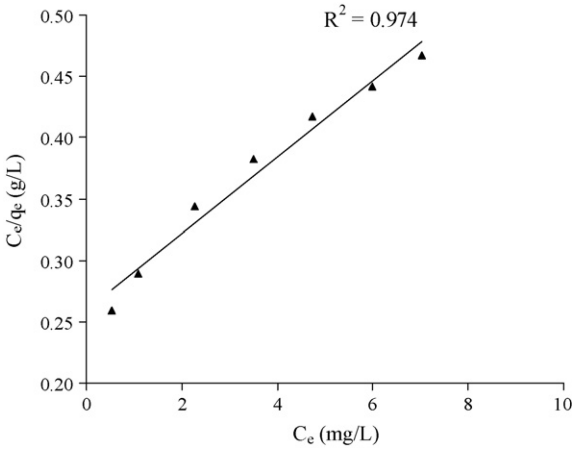

Fig. 6. The Langmuir Adsorption isotherm of RB 15 dye onto the Turkish Sepiolite. Contact time 3 h, temperature 295.15 K.

Table 3
Langmuir and Freundlich parameters for the adsorption of RB 15 dye onto the Turkish Sepiolite sample

Dye	Langmuir			Freundlich		
	q_m (mg/g)	K_L (l/g)	R^2	n	K_f (mg $^{(1-1/n)}$ $L^{1/n}$/g)	R^2
RB 15	31.98	0.12	0.974	1.29	3.43	0.999

form of Langmuir model (Eq. (2)) [32] as follows:

$$\frac{C_e}{q_e} = \frac{C_e}{q_m} + \frac{1}{K_L q_m} \quad (2)$$

where C_e is the equilibrium concentration of dye (mg/l) and q_e is the amount of the dye adsorbed (mg) by per unit of sepiolite (g). q_m and K_L are the Langmuir constants related to the adsorption capacity (mg/g) and the equilibrium constant (l/g), respectively. The Langmuir monolayer adsorption capacity (q_m) gives the amount of the dye required to occupy all the available sites per unit mass of the sample. The Langmuir monolayer adsorption capacity of RB 15 dye was estimated as 31.98 mg/g (Table 3). The adsorption capacity of the sepiolite for the removal of anionic dye has been compared with that of other adsorbents reported in literature. The values reported in the form of monolayer adsorption capacity. The experimental data of the present investigation are comparable with the reported values. For example, adsorption of Everzol Red 3BS on the sepiolite follows the Langmuir isotherm model with an adsorption capacity of 108.8 mg/g [33]. Huang et al. [34] have reported a Langmuir monolayer capacity, q_m, of 91.74 mg/g at for Reactive Red MF-3B onto organoclay. Langmuir adsorption capacity for Reactive Black 5 adsorption on powdered activated carbon and fly ash has been shown to be 58.82 and 7.93 mg/g, respectively [35]. The uptake of reactive dye RR 222 on activated clay has Langmuir monolayer capacity q_m = 36.4 mg/g [36]. Wu [37] found the Langmuir adsorption capacity for reactive dye onto carbon nanotubes as 39.84 mg/g at pH 6.5 and 301 K. The comparison of q_m value of the Turkish Sepiolite used in the present study with those obtained in the literature shows that the Turkish Sepiolite is as effective as other adsorbents.

The adsorption equilibrium data was also applied to the Freundlich model (Eq. (3)) [38]:

$$\log q_e = \log K_f + \left(\frac{1}{n}\right) \log C_e \quad (3)$$

where K_f and n are Freundlich constants related to adsorption capacity and adsorption intensity, respectively. Freundlich parameters (K_f and n) indicate whether the nature of adsorption is either favourable or unfavourable. The intercept and slope are indicators of adsorption capacity and intensity, respectively. A relatively slight slope $n \ll 1$ indicates that adsorption intensity is good (or favourable) over the entire range of concentrations studied. Adsorption intensity is good (or favourable) at high concentrations while a steep slope ($n > 1$), but much less at lower concentrations. A high value of the intercept, K_F, is indicative of a high adsorption capacity. In the RB 15 dye adsorption system, n value is 3.43, which indicates that adsorption intensity is good (or favourable) over the entire range of concentrations studied. The K_F value of the Freundlich equation (Table 3) also indicates that RB 15 dye has a very high adsorption capacity in aqueous solution.

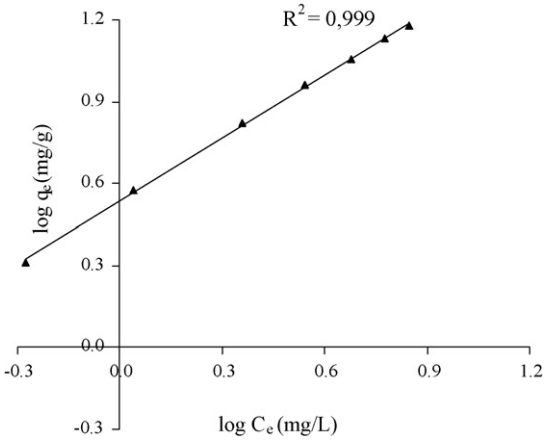

Fig. 7. The Freundlich adsorption isotherm of RB 15 dye onto the Turkish Sepiolite. Contact time 3 h, temperature 295.15 K.

3.2. IR spectroscopic and surface area analysis of adsorbed dyes species on the Turkish Sepiolite

In the case of interactions between organic molecules and clays such as sepiolite, smectite, vermiculite, etc., the adsorbed these molecules may be either coordinated to oxygen plane (Si–O–Si) through water molecules or displaced the same water molecules from sphere of the coordination to take place a direct linkage exchangeable cation in the interlayer [15]. In the case of the IR spectra of the untreated Turkish Sepiolite and the dye composites of Turkish Sepiolite (for OH stretching regions), the shift of the broad OH stretching band from 3451 to 3440 cm^{-1} (Fig. 8a) and the observed sharpness, and also appearance of additional N–H stretching band at 3490 cm^{-1} (Fig. 8b) should be an evidence that

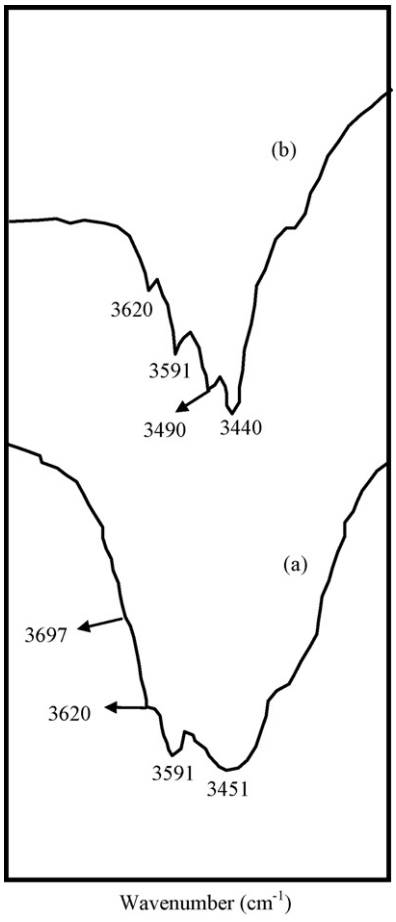

Fig. 8. (a) The IR spectra of the untreated Turkish Sepiolite and (b) the Turkish Sepiolite-dye composite.

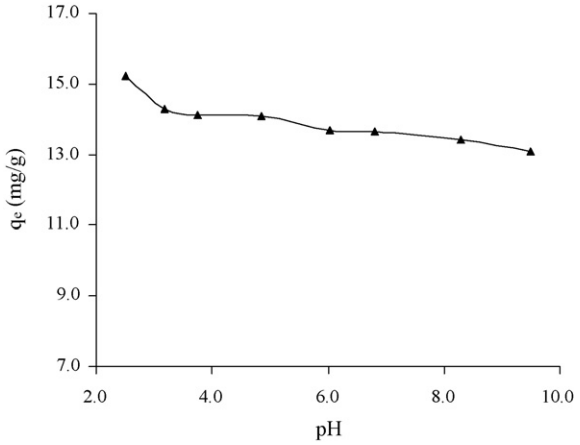

Fig. 9. Effect of initial pH for the adsorption of RB 15 dye onto the Turkish Sepiolite. T = 295.15 K, initial pH 6.0, m = 2 g/L, C_0 = 20 mg/L.

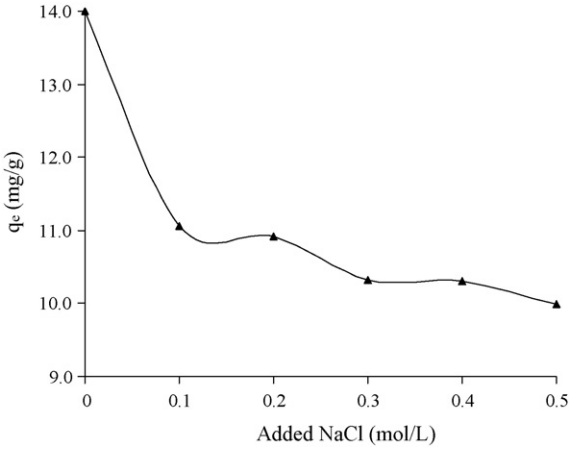

Fig. 10. Effect of solution ionic strength on the adsorption of RB 15 dye onto the Turkish Sepiolite. T = 295.15 K, initial pH 6.0, m = 2 g/L, C_0 = 20 mg/L.

these species replaced partly the zeolitic water which is hydrogen-bonded to bound water.

From IR data it was concluded that the interaction between the RB 15 dye molecules and the Turkish Sepiolite was through its N–H group.

The dimensions of channels for the sepiolite are usually about 10.6 × 3.7 Å [17]. In the case of the large RB 15 dye molecule, where 3D picture of its for which the height determined from the bonds lengths as ~10 Å points out that its entry into the Turkish Sepiolite channels is prohibited. It was from geometrical consideration of this dye molecule concluded that dye species adsorb to the channels sites [22]. Decrease of the surface area of the untreated Turkish Sepiolite (274 $m^2\,g^{-1}$) to 82 $m^2\,g^{-1}$ for the Turkish Sepiolite-dye composite may be taken as another proof for this result. The decrease in the surface area of the Turkish Sepiolite-dye composite may be explained in terms of the micropore openings blocked by the dye species adsorbed to the channels sites which form a macroporous structure [39].

3.3. Initial pH and ionic strength effects on the adsorption of dyes

The effect of initial pH of dye solution on removal of the dye is shown in Fig. 9. At pH, ranging from 2.5 to 9.5, the effect of initial pH on the dye removal was slight, and the final pH values were all stabilized around 7.2. The slight effect of pH on the dye removal as well as high and stable final pH of the suspensions is mainly determined by the nature of large pH buffer capacity of sepiolite suspension. Therefore, pH is not a critical limiting factor in pursuing a high efficiency of the dye removal using sepiolite and no rigid pH control is needed. That is an important advantage for sepiolite application because dye removal using conventional adsorbents or chemical coagulants is strongly pH-dependent and thereby an optimal pH condition should be remained to achieve a satisfactory result. As seen from these figures, it was observed that the amount of this adsorbed dye increased below pH 3.0. This result is closely related to the surface charge of the adsorbent and the degree of ionization of adsorbate. At low pH (pH < 3.0), the surface of sepiolite becomes positively charged, whereas the solution/sepiolite interface and its surface at gradual higher pH appear neutral or negatively charged due to the deprotonation of the surface. The electrostatic attraction between positively charged adsorption sites and negatively charged dye anions for pH values lower than ~3.0 causes an increase in the adsorbed amount of dye, but the electrostatic repulsion between the two groups with different charge for the higher pH dominates. As a result, while the little increase in the positively charged sites on the sepiolite for the adsorption of this anionic dye is the driving power at strong acidic pH. Nevertheless, significant adsorption of the anionic dye on the adsorbent still occurred at high pH values due to the fact that a chemical interaction between RB 15 dye and the Turkish Sepiolite taken place. This was further proved by the change in the FTIR spectra of the Turkish Sepiolite before and after dye adsorption (Section 3.2). The interaction of the anionic dye with the surface of the sepiolite material is expected to be mainly between the Lewis acid sites, which are related to delocalized π electrons on the surfaces of the sepiolite, and (i) the free electrons of the dye molecule resulting from several aromatic rings and double bonds; (ii) the negatively charged ion of the dye. The significant adsorption of the anionic dye on the sepiolite at high pH values can be attributed to the fact that Lewis acid sites attract and thus localize π electrons of the condensed aromatic sheets on the surface of this adsorbent.

The ionic strength effect of the medium on the adsorption ability of the Turkish Sepiolite sample towards dyes at pH 6.0 was investigated using NaCl solutions from 0 to 0.5 M. As seen in Fig. 10, increasing the ionic strength of the solution causes the decrease in the adsorption of dye onto Turkish Sepiolite surface. The amount of adsorbed dye by sepiolite sample decreases parallelly with the increase in the ionic strength of the medium. This result can be explained by the reduction in the positive surface potential of the Turkish Sepiolite sample [40,41].

3.4. Effect of temperature on adsorption

Using the following equations, the thermodynamic parameters of the adsorption process were determined from the experimental data:

$$\ln K_d = \frac{\Delta S}{R} - \frac{\Delta H}{RT} \quad (4)$$

$$\Delta G = \Delta H - T\,\Delta S \quad (5)$$

$$K_d = \frac{q_e}{C_e} \quad (6)$$

where K_d is the distribution coefficient for the adsorption, ΔS, ΔH and ΔG are the changes of entropy, enthalpy and the Gibbs energy, T (K) is the temperature, R (J/mol K) is the gas constant. The values of ΔH and ΔS were determined from the slopes and intercepts of the plots of $\ln K_d$ vs. $1/T$ (not showed).

As given in Table 4, the adsorption of the RB 15 dye onto the Turkish Sepiolite sample is an endothermic process, which indicates that the amount of the adsorbed dye increases at higher tempera-

Table 4
Thermodynamic data for adsorption of RB 15 dye onto the Turkish Sepiolite sample

Sample	ΔH (kJ/mol)	ΔS (J/mol K)	ΔG (kJ/mol)				R^2
			298.15 K	313.15 K	323.15 K	333.15 K	
RB 15	1.95	15.0	−2.52	−2.75	−2.90	−3.05	0.98

tures. This result may be explained with increase in the mobility of the large dye molecules depending on increase in temperature and a number of these molecules to interact adsorption cites. Subsequently, the increasing mobility of dye molecules. Moreover, the alteration of temperature from room temperature to 55 °C may induce a swelling effect within the internal structure of the sepiolite enabling the same molecules to penetrate further. The endothermic process also supports the possibility of bonding between the adsorbate and the sepiolite product. Thus, it was concluded that the amin (NH_2) groups of dye might interact with acid oxide sites on the Turkish Sepiolite.

The ΔG and ΔS values for adsorption of reactive dye are given in Table 4. The nature of adsorption process is spontaneous due to the negative values of ΔG, and also the positive ΔS values for the same process are in parallel with the result. The positive ΔS value shows that the RB 15 dye and the Turkish Sepiolite surface impose a new and ordered structure on the surrounding water molecules. The decrease in the number of water molecules surrounding the dye molecules and the positive value of ΔS, point out the increased randomness at solid–solution interface during the adsorption of this dye on the Turkish Sepiolite. Furthermore, values of T_{av} ΔS can be calculated from the experimental data where T_{av} represents the average values of the range of temperature used for adsorption studies. It is found that $\Delta H < T_{av}$ ΔS for the sepiolite. This means, although contribution of ΔH are not negligible, but the influence of entropies are more remarkable. The negative ΔG values indicate that the adsorption process is thermodynamically feasible at room temperature.

Thermodynamic data on anionic dye adsorption on different adsorbents are scarce. Abdelwahab [42] reported the thermodynamic parameters for adsorption of reactive orange on loofa-activated carbons (LC). ΔH and ΔS values were −14.2 kJ/mol and +8.59 J/mol K for LC1, −17.93 kJ/mol and +13.65 J/mol K for LC2. Dizge et al. [43] reported that ΔH and ΔS for adsorption of Remazol Red onto fly ash has values of +13.93 kJ/mol and +63 J/mol K, respectively. Dai [44] investigated the adsorption of carmine and titan yellow onto activated carbon. The values of ΔH, and ΔS were reported as −130 kJ/mol and −1.4 J/mol K for carmine at pH 3.5 and −13 kJ/mol and −5.0 J/mol K, respectively, for titan yellow at pH 3.5. Gupta et al. [45] have reported that ΔH and ΔS for adsorption of Naphthol red-J onto nontronite mineral has values of +20.50 kJ/mol, and 76 J/mol K at pH 4,and 4.25 kJ/mol and 20 J/mol K at pH 9, respectively. These values are not much different from the values obtained in this work.

3.5. Adsorption kinetic

Several kinetic models are available to understand the behaviour of the adsorbent and to examine the controlling mechanism of the adsorption process and also to test the experimental data. In the present investigation, the adsorption data were analyzed using three kinetic models: the pseudo-first-order, pseudo-second-order kinetic and the intraparticle diffusion models.

The pseudo-first-order model was presented by Lagergren [46]. The Lagergren's first-order reaction model is expressed as follows by Gürses et al. [47] and El-Khaiary [48]:

$$\frac{dq_t}{dt} = k_1(q_e - q_t) \tag{7}$$

where q_e and q_t are the amounts of dye (mmol/g) adsorbed on the clay at equilibrium, and at time t, respectively and k_1 is the rate constant (min^{-1}). Integrating and applying the boundary condition ($t = 0$ and $q_t = 0$) to ($t = t$ and $q_e = q_t$), Eq. (7) takes the form:

$$\log(q_e - q_t) = \log q_e - \left(\frac{k_1}{2.303}\right) t \tag{8}$$

The rate constant k_1 was obtained from slope of the linear plots of $\log(q_e - q_t)$ against t.

The sorption data was also analyzed in terms of pseudo-second-order mechanism, described in Refs. [47,48]:

$$\frac{dq_t}{dt} = k_2(q_e - q_t)^2 \tag{9}$$

where k_2 is the rate constant of pseudo-second-order sorption (g/mg min). Integrating and applying boundary conditions ($t = 0$ and $q_t = 0$) to ($t = t$ and $q_e = q_t$), Eq. (9) becomes

$$q_t = \frac{t}{(1/k_2 q_e{}^2) + (1/q_e)} \tag{10}$$

which has linear form as

$$\frac{1}{q_t} = \frac{1}{k_2 q_e{}^2 + (1/q_e)t} \tag{11}$$

If initial adsorption rate [47,48] is

$$h = k_2 q_e{}^2 \tag{12}$$

then Eqs. (10) and (11) become

$$q_t = \frac{t}{(1/h) + (1/q_e)} \tag{13}$$

and

$$\frac{t}{q_t} = \frac{1}{h} + \frac{1}{q_e}t \tag{14}$$

If second-order kinetics is applicable, the plot of t/q_t against t should give a linear relationship from which the constants $q_e h$ and k_2 can be determined.

Table 5 lists the results of the rate constant studies for different initial pH values by the pseudo-first-order and pseudo-second-order models at 295.15 K. It is seen that the correlation coefficient of pseudo-first-order kinetic are lower than that of the pseudo-second-order kinetic model. This finding shows that kinetics of the dye adsorption by the Turkish Sepiolite is better described by pseudo-second-order kinetic model rather than pseudo-first-order model. For the pseudo-second-order model in Table 5, the rate constant for the dye generally decreased with the increase of the initial pH value. At lower pH values, dye ions present in the adsorption medium could interact with the binding sites, hence higher rate constant results. At higher pH values, the rate constant of the dye adsorption onto the Turkish Sepiolite shows a decreasing trend due to the ionization of the adsorption sites.

Table 5
Kinetic parameters for the adsorption of RB 15 dye onto the Turkish Sepiolite sample at different initial pH values

	pH	Pseudo-first-order model		Pseudo-second-order model			
		R_1^2	k_1 ($\times 10^3$ min^{-1})	R_2^2	q_e (mg/g)	h (mg/g min)	k_2 ($\times 10^2$ g/mg min)
RB 15	3	0.684	5.46	0.999	5.97	3.97	11.13
	5	0.643	4.65	0.999	5.03	1.99	7.85
	9	0.880	8.12	0.999	3.95	0.63	3.99

4. Conclusions

The results of the adsorptions of RB 15 dye species on the Turkish Sepiolite demonstrated that the functional groups of adsorbate and water molecules of adsorbent played an active role. The data obtained Fourier transform infrared (FTIR) and surface area measurement techniques indicated that the RB 15 dye molecules adsorb to the channels sites of the Turkish Sepiolite. The increase in the adsorbed amount depending on the decrease in the pH of dye–clay suspensions imparted the increase of the electrostatic attraction between positively charged adsorptive sites and negatively charged dye anions. In addition, the alterations of the ionic strength of the solutions were in agreement with this result. The cause of increasing of adsorbed amount with decreasing ionic strength is that; increase in the ionic strength, increases the negative charge of the surface, resulting in greater repulsive of dye anions. In the case of the increasing temperature, the observed positive enthalpy change points out the possibility of bonding the adorbate and adsorbent. Furthermore, the negative values of ΔG and positive ΔS value showed that the nature of adsorption process was the spontaneous.

References

[1] H. Øllgaard, L. Frost, J. Galster, O.C. Hansen, Survey of Azo-colorants in Denmark: Consumption, Use Health and Environmental Aspects, Ministry of Environment and Energy, Denmark, 1998.
[2] T. Robinson, G. McMullan, R. Marchant, P. Nigam, Remediation of dyes in textile effluent: a critical review on current treatment technologies with a proposed alternative, Bioresour. Technol. 77 (2001) 247–255.
[3] O. Tünay, I. Kabdasli, G. Eremektar, D. Orhon, Color removal from textile wastewaters, Water Sci. Technol. 34 (1996) 9–16.
[4] N.M. Mahmoodi, M. Arami, N.Y. Limaee, Photocatalytic degradation of triazinic ring-containing azo dye (Reactive Red 198) by using immobilized TiO_2 photoreactor: Benc scale study, J. Hazard. Mater. B 133 (2006) 113–118.
[5] T.N.C. Dantas, L.T.C. Beltrame, A.A.D. Neto, M.C.P.A. Moura, Use of microemulsions for removal of color and dyes from textile wastewater, J. Chem. Technol. Biotechnol. 79 (2004) 645–650.
[6] M.S. Khehra, H.S. Saini, D.K. Sharma, B.S. Chadha, S.S. Chimni, Decolorization of various azo dyes by bacterial consortium, Dyes Pigments 67 (2005) 55–61.
[7] S. Netpradit, P. Thiravetyan, S. Towprayoon, Adsorption of three azo reactive dyes by metal hydroxide sludge: effect of temperature, pH, and electrolytes, J. Colloid Interface Sci. 270 (2004) 255–261.
[8] S.D. Lambert, N.J.D. Graham, C.J. Sollars, G.D. Fowler, Evaluation of inorganic adsorbents for the removal of problematic textile dyes and pesticides, Water Sci. Technol. 36 (1997) 173–180.
[9] F.C. Wu, R.L. Tseng, r.S. Juang, Kinetics of color removal by adsorption from water using activated clay, Environ. Technol. 22 (2001) 721–729.
[10] I.A. Balcioglu, I. Arslan, M.T. Sacan, Homogenous heterogenous advanced oxidation of two commercial reactives dyes, Environ. Technol. 22 (2001) 813–822.
[11] D. Gonzalez-Roman, M.D. Ruiz-Cruz, R. Pozas-Tormo, J.R. Ramos-Barrodo, C. Criado, L. Moreno-Real, Ionic conduction in sepiolite, Solid State Ionics 61 (1993) 163–172.
[12] S. Akyüz, T. Akyüz, J.E.D. Davies, An FT-IR spectroscopic investigation of the adsorption of benzidine by sepiolite from Eskisehir (Turkey), J. Mol. Struct. 293 (1993) 279–282.
[13] M. Myriam, M. Suarez, J.M. Martin-Pozas, Structural textural modification of palygorskite and sepiolite under acid treatment, Clays Clay Miner. 3 (1998) 225–231.
[14] S. Akyüz, T. Akyüz, Infrared spectral investigations of adsorption and oxidation of *N*,*N*-dimethylaniline by sepiolite, loughlinite and diatomite, J. Inclus. Phenom. 5 (1987) 259–262.
[15] S. Yariv, Thermo-IR-spectroscopy analysis of the interactions between organic pollutants and clay minerals, Thermochim. Acta 274 (1996) 1–35.
[16] Y. Grillet, J.M. Cases, M. Francois, J. Rouquerol, J.E. Poirier, Modification of the porous structure and surface area of sepiolite under vacuum thermal treatment, Clays Clay Miner. 36 (1988) 233–242.
[17] S. Argast, Expandable sepiolite from Ninetyeast Ridge, Indian Ocean, Clays Clay Miner. 37 (1989) 371–376.
[18] G. Brown, Crystal structures of clay minerals and related phylosilicates in clay minerals: their structure behaviour and use, in: Proceedings of a Royal Society Discussion Meeting, November 9 and 10, 1983, organized and edited by Sir L. Fowden, R.M. Barrer, P.B. Tınker.
[19] U. Shuali, L. Bram, M. Steinberg, S. Yariv, Catalytic thermal reactions of cumene over sepiolite and palygorskite, J. Therm. Anal. 37 (1991) 1569–1578.
[20] H. Shariatmadari, A.R. Mermut, M.B. Benke, Sorption of selected cationic and neutral organic molecules on palygorskite and sepiolite, Clays Clay Miner. 47 (1999) 44–53.
[21] H. Ceylan, A. Yıldız, Y. Sarıkaya, Investigation of the adsorption of fatty acids on two different clays using IR, DTA and TGA techniques, Doga-Tr. J. Chem. 17 (1993) 267–272.
[22] G. Rytwo, S. Nir, L. Margulies, B. Casal, J. Merino, E. Ruiz-Hitzky, J.M. Serratosa, Adsorption of monovalent organic cations on sepiolite: experimental results and model calculations, Clays Clay Miner. 46 (1998) 340–348.
[23] G. Atun, G. Hisarli, A Study of surface properties of red mud by potentiometric method, J. Colloid Interface Sci. 228 (2000) 40–45.
[24] M. Yeniyol, Vein-like sepiolite occurrence as a replacement of magnesite in Konya, Turkey, Clays Clay Miner. 34 (1986) 353–356.
[25] U. Shuali, L. Bram, M. Steinberg, S. Yariv, Infrared study of the thermal treatment of sepiolite and palygorskite saturated with organic amines, Thermochim. Acta 148 (1989) 445–456.
[26] J. Cornejo, M.C. Hermosin, Structural alteration of sepiolite by dry grinding, Clay Miner. 23 (1988) 391–398.
[27] M. Duc, F. Thomas, F. Gaboriaud, Coupled chemical processes at clay/electrolyte interface: a batch titration study of Na-montmorillonites, J. Colloid Interface Sci. 300 (2006) 616–625.
[28] M. Duc, F. Gaboriaud, F. Thomas, Sensitivity of the acid–base properties of clays to the methods of preparation and measurement. 2. Evidence from continuous potentiometric titrations, J. Colloid Interface Sci. 289 (2005) 148–156.
[29] F.R.C. Chang, G. Sposito, The electrical double layer of a disk-shaped clay mineral particle: effect of particle size, J. Colloid Interface Sci. 163 (1994) 19–27.
[30] M.J. Avena, M.M. Mariscal, C.P. De Pauli, Proton binding at clay surfaces in water, Appl. Clay Sci. 24 (2003) 3–9.
[31] A.M.L. Kraepiel, K. Keller, F.M.M. Morel, A model for metal adsorption on montmorillonite, J. Colloid Interface Sci. 210 (1999) 43–54.
[32] I. Langmuir, The adsorption of gases on plane surfaces of glass, mica and platinum, J. Am. Soc. 40 (1918) 1361–1403.
[33] O. Ozdemir, B. Armagan, M. Turan, M.S. Çelik, Comparison of the adsorption characteristics of azo-reactive dyes on mezoporous minerals, Dyes Pigments 62 (2004) 49–60.
[34] J. Huang, Y. Liu, Q. Jin, X. Wang, J. Yang, Adsorption studies of a water soluble dye, Reactive Red MF-3B, using sonication-surfactant-modified attapulgite clay, J. Hazard. Mater. 143 (2007) 541–548.
[35] Z. Eren, F.N. Acar, Adsorption of Reactive Black 5 from an aqueous solution: equilibrium and kinetic studies, Desalination 194 (2006) 1–10.
[36] M.-Y. Chang, R.-S. Juang, Adsorption of tannic acid, humic acid, and dyes from water using the composite of chitosan and activated clay, J. Colloid Interface Sci. 278 (2004) 18–25.
[37] C.-H. Wu, Adsorption of reactive dye onto carbon nanotubes: equilibrium, kinetics and thermodynamics, J. Hazard. Mater. 144 (2007) 93–100.
[38] H. Freundlich, Über die adsorption in lösungen, Z. Phys. Chem. (Leipzig) 57 (1906) 385–470.
[39] A. Tabak, B. Afsin, B. Caglar, E. Koksal, Characterization and pillaring of a Turkish bentonite (Resadiye), J. Colloid Interface Sci. 313 (2007) 5–11.
[40] Y.G. Mishael, G. Rytwo, S. Nir, M. Crespin, F. Annabi-Bergaya, H. Van Damme, Interactions of monovalent organic cations with pillared clays, J. Colloid Interface Sci. 209 (1999) 123–128.
[41] M. Alkan, O. Demirbas, S. Celikcapa, M. Dogan, Sorption of acid red 57 from aqueous solution onto sepiolite, J. Hazard. Mater. 116 (2004) 135–145.
[42] O. Abdelwahab, Evaluation of the use of loofa activated carbons as potential adsorbents for aqueous solutions containing dye, Desalination 222 (2008) 357–367.
[43] N. Dizge, C. Aydiner, E. Demirbas, M. Kobya, S. Kara, Adsorption of reactive dyes from aqueous solutions by fly ash: kinetic and equilibrium studies, J. Hazard. Mater. 150 (2008) 737–746.

[44] M. Dai, Mechanism of Adsorption for dyes on activated carbon, J. Colloid Interface Sci. 198 (1998) 6–10.
[45] V.K. Gupta, D. Mohan, V.K. Saini, Studies on the interaction of some azo dyes (naphthol red-J and direct orange) with nontronite mineral, J. Colloid Interface Sci. 298 (2006) 79–86.
[46] S. Lagergren, Zur theorie der sogenannten adsorption gelöster stoffe, Kungliga Svenska Vetenskapsakademiens, Handlingar 24 (1898) 1–39.
[47] A. Gürses, Ç. Doğar, M. Yalçın, M. Açıkyıldız, R. Bayrak, S. Karaca, The adsorption kinetics of the cationic dye, methylene blue, onto clay, J Hazard. Mater. 131 (2006) 217–228.
[48] M.I. El-Khaiary, Kinetics and mechanism of adsorption of methylene blue from aqueous solution by nitric-acid treated water-hyacinth, J Hazard. Mater. 147 (2007) 28–36.